



University of Pennsylvania  
ScholarlyCommons

---

Departmental Papers (MSE)

Department of Materials Science & Engineering

---

November 2001

# Structure and properties of $C_{60}@SWNT$

Brian W. Smith  
*University of Pennsylvania*

Richard M. Russo  
*University of Pennsylvania, rrusso@seas.upenn.edu*

Satishkumar B. Chikkannanavar  
*University of Pennsylvania, satishkb@seas.upenn.edu*

Ferenc Stercel  
*University of Pennsylvania, stercel@seas.upenn.edu*

David E. Luzzi  
*University of Pennsylvania, luzzi@lrsm.upenn.edu*

Follow this and additional works at: [http://repository.upenn.edu/mse\\_papers](http://repository.upenn.edu/mse_papers)

---

## Recommended Citation

Smith, B. W., Russo, R. M., Chikkannanavar, S. B., Stercel, F., & Luzzi, D. E. (2001). Structure and properties of  $C_{60}@SWNT$ . Retrieved from [http://repository.upenn.edu/mse\\_papers/17](http://repository.upenn.edu/mse_papers/17)

Copyright Materials Research Society. Reprinted from MRS Proceedings Volume 706.  
2001 Fall Meeting Symposium Z  
Making Functional Materials with Nanotubes  
Publisher URL: [http://www.mrs.org/members/proceedings/fall2001/z/Z6\\_20.pdf](http://www.mrs.org/members/proceedings/fall2001/z/Z6_20.pdf)

This paper is posted at ScholarlyCommons. [http://repository.upenn.edu/mse\\_papers/17](http://repository.upenn.edu/mse_papers/17)  
For more information, please contact [libraryrepository@pobox.upenn.edu](mailto:libraryrepository@pobox.upenn.edu).

---

# Structure and properties of C<sub>60</sub>@SWNT

## **Abstract**

Our recent achievement of high-yield C<sub>60</sub>@SWNT synthesis facilitates characterization by various techniques, including selected area electron diffraction (SAD) and Raman spectroscopy. The obtained SAD patterns show that interior C<sub>60</sub> molecules sit on a simple 1-D lattice having a parameter of 1.00 nm. Simulated SAD patterns and real-space measurements both support this determination and do not indicate a lattice with a more complex basis, e.g. a dimer basis. Empty and bulk-filled SWNTs (22%, 56%, and 90% yields), each subjected to identical processing steps, were examined by room temperature Raman spectroscopy. Systematic differences are seen between the spectra of filled and unfilled SWNTs, particularly with respect to the G- and RBM-bands of the nanotubes. We present a possible explanation for this behavior.

## **Comments**

Copyright Materials Research Society. Reprinted from MRS Proceedings Volume 706.

2001 Fall Meeting Symposium Z

Making Functional Materials with Nanotubes

Publisher URL: [http://www.mrs.org/members/proceedings/fall2001/z/Z6\\_20.pdf](http://www.mrs.org/members/proceedings/fall2001/z/Z6_20.pdf)

## Structure and properties of C<sub>60</sub>@SWNT

Brian W. Smith, Richard M. Russo, S.B. Chikkannanavar, Ferenc Stercel, David E. Luzzi  
University of Pennsylvania, Department of Materials Science and Engineering,  
3231 Walnut Street, Philadelphia, PA 19104-6272, USA

### ABSTRACT

Our recent achievement of high-yield C<sub>60</sub>@SWNT synthesis facilitates characterization by various techniques, including selected area electron diffraction (SAD) and Raman spectroscopy. The obtained SAD patterns show that interior C<sub>60</sub> molecules sit on a simple 1-D lattice having a parameter of 1.00 nm. Simulated SAD patterns and real-space measurements both support this determination and do not indicate a lattice with a more complex basis, e.g. a dimer basis. Empty and bulk-filled SWNTs (22%, 56%, and 90% yields), each subjected to identical processing steps, were examined by room temperature Raman spectroscopy. Systematic differences are seen between the spectra of filled and unfilled SWNTs, particularly with respect to the G- and RBM-bands of the nanotubes. We present a possible explanation for this behavior.

### INTRODUCTION

The single wall carbon nanotube has garnered fame for its potential to become a seminal engineering material. Intrinsicly, a SWNT exhibits remarkable mechanical and electronic properties that make it suitable for use in a broad range of envisaged commercial applications. What is often overlooked, however, is that nanotubes might be selectively modified to improve upon these same properties. For example, the fact that a nanotube encloses an essentially one-dimensional lumen opens the possibility for using it as a template to nanostructure atoms, ions, or small molecules into linear arrangements. Certain one-dimensional phenomena have been treated theoretically, but few 1-D systems are known to exist in reality. For this reason, little is known about how materials behave in one-dimension. Indeed, such materials might prove to be extraordinarily important.

Presently, the paradigm one-dimensional material is C<sub>60</sub>@SWNT: a linear array of C<sub>60</sub> molecules enclosed by a SWNT via van der Waals interactions. Since its discovery [1] and high-yield synthesis [2], the structure of C<sub>60</sub>@SWNT has been widely debated. Similarly controversial has been the question of whether the electronic states of the SWNT are perturbed by the presence of interior C<sub>60</sub>. In this letter, we present a solution to the structure of C<sub>60</sub>@SWNT using empirical and simulated electron diffraction. We also compare Raman spectra of bulk SWNT material containing filled and empty nanotubes. Our data show systematic differences that are not inconsistent with changes in the measured vibronic states upon filling.

### EXPERIMENTAL DETAILS

C<sub>60</sub>@SWNT was synthesized in milligram aliquots using methods that are described elsewhere, i.e. in ref. [2]. At the time of synthesis, a separate batch of control samples were

subjected to the same chemical and thermal processing steps, but no C<sub>60</sub> was introduced and so the control SWNTs remained empty. Benchmarking the experimental (filled) samples against these control samples enabled the yield of C<sub>60</sub>@SWNT to be determined for each processing condition. The experiments described herein utilized SWNTs filled with C<sub>60</sub> to 22%, 56%, and 90% by length. Nominally, each sample was a thin mat of entangled SWNT ropes.

### **Selected area diffraction**

A piece of the 90% material was torn away from the mat and fixed to a folding TEM grid. At the tear, SWNT ropes are pulled from the bulk and can be imaged without the use of a support film. The sample was imaged in a JEOL 2010F operated at 100 kV. Diffraction patterns were recorded from ropes appearing linear and focused across the entire breadth of a 1 μm selected area aperture. To minimize thermal effects, the sample was maintained at 94 K using a Gatan cooling stage during the data collection process. Simulated diffraction patterns were calculated directly using the Mathematica software package.

### **Raman spectroscopy**

Raman spectra were recorded at room temperature using a 514.5 nm (green) laser focused to a 1 μm illumination spot. Spectra were recorded from 10-20 randomly selected locations on each of the 22%, 56%, and 90% control and experimental samples (6 samples total). All spectra were qualitatively similar, exhibiting two sharp peaks in the G-band at ~1590 and ~1565 cm<sup>-1</sup>, a weak D-band centered at ~1345 cm<sup>-1</sup>, and an RBM band centered at ~185 cm<sup>-1</sup> with a shoulder to the Stokes side. Each of these bands is a known feature in the Raman spectrum of SWNT material (for example, see [3]). We denote these peaks G<sub>1</sub>, G<sub>2</sub>, D, and R.

In the present work, we do not attempt to deconvolute our spectra into their Lorentzian components. Instead, we examine the full-maximum intensities of the G<sub>1</sub>, G<sub>2</sub>, D, and R peaks. Absolute intensities from different spectra cannot be easily compared due to differences in illumination condition, sample density, etc. However, a homogeneous sample should show little variation in the normalized intensities (G<sub>1</sub>/D, G<sub>2</sub>/D, R/D) as a function of location. In all six of the analyzed samples, these have a standard deviation of only 5-10%.

## **RESULTS AND DISCUSSION**

Our discussion of the pattern in Figure 1 is facilitated by defining the meridian (oriented horizontally) and the equator (oriented vertically) as the reciprocal space axes parallel and perpendicular to the predominant direction of the real space rope axis, respectively. In addition to the usual rope lattice and graphene lattice reflections, an additional set of reflections is visible. These appear as broken streaks, centered about the meridian and spaced by 0.629 Å<sup>-1</sup>, using the known graphene lattice reflections that fall on the same axis as a basis for comparison. The corresponding real space periodicity is 0.998 nm — almost exactly equal to the <110> (close packed) intermolecular separation in fcc C<sub>60</sub> (1.004 nm). This value is consistent with our real space measurement of C<sub>60</sub>-C<sub>60</sub> separation (0.97 nm), since any tilt of the rope out of the object plane will lead to smaller perceived separations in the projected image.

In Figure 1, the radial width of the 1-D lattice reflections is equal to that of the graphene lattice reflections, indicating that the coherence lengths of the SWNTs and of the 1-D  $C_{60}$  crystals are essentially the same. That is, the widths of the reflections support that the SWNTs are filled over at least a 1 micron length. Since each pattern arises from scattering off multiple, straight and parallel  $C_{60}$ @SWNT monocrystals that compose the rope, the area selected by the aperture can be regarded as a representative sampling of the bulk material. It would be extremely unlikely that the scattering SWNTs would be well-filled only in the area of the aperture. Therefore, it is not unreasonable to conclude that each tube is *actually* filled over its entire length. Both the diffraction data and the images suggest a simple lattice interpretation of the structure.

Further support of this interpretation is obtained by a simple calculation of the pattern expected from a 1-D chain of  $C_{60}$  molecules. We define the reciprocal space axes ( $u, v, w$ ) parallel to the real space axes ( $x, y, z$ ). To a first approximation,  $C_{60}$  is a homogeneous spherical shell of charge having radius  $r = 3.5 \text{ \AA}$ . Its molecular form factor  $\phi(Q)$  is also spherically symmetric. As a function of radial distance  $Q$  (i.e. in one-dimension), it is equal to the zero-order spherical Bessel function  $j_0(Qr) = \sin(Qr)/Qr$ , where  $Q = \sqrt{u^2 + v^2 + w^2}$ .

Now consider the case where many  $C_{60}$  molecules are arranged into a one-dimensional lattice along the  $x$  axis. The 1-D lattice having lattice constant  $a = 1.0 \text{ nm}$  can be represented by an array of delta functions. For a finite 1-D lattice having  $N = 2M + 1$  elements, this array can be described in *three dimensions* by the following function:

$$\Lambda(x, y, z) = \sum_{n=-M}^M \delta(x - na) \delta(y) \delta(z) \quad (1)$$

$n$  is an integer index, and  $\delta$  is the Dirac delta function. The crystal is therefore composed of the lattice convoluted with a  $C_{60}$  basis. We are interested in the scattering amplitude,  $\sigma = \mathfrak{F}\{\Lambda \otimes C_{60} \text{ basis}\}$ . By the convolution theorem,  $\sigma = \mathfrak{F}\{\Lambda\} \mathfrak{F}\{C_{60} \text{ basis}\}$ :

$$\sigma(u, v, w) = \frac{\sin\left(\frac{Nua}{2}\right)}{\sin\left(\frac{ua}{2}\right)} \frac{\sin\left(r\sqrt{u^2 + v^2 + w^2}\right)}{r\sqrt{u^2 + v^2 + w^2}} \quad (2)$$

If the electron beam is directed down the  $z$  axis, then the Ewald sphere slices through  $\sigma(u, v, w)$  along the plane  $w = 0$ . Setting  $w = 0$  and choosing a typical coherence length of  $N = 1000$  molecules (corresponding to a  $1 \text{ \mu m}$  selected area aperture), we calculate  $f(Q)^2 \sigma(Q)^2$ , which is proportional to the observed SAD intensity. Tabulated values of  $f(Q)$ , the atomic scattering factor for carbon, were utilized.

A simulated SAD pattern for the periodic 1-D chain appears in Figure 2. The response of the electron microscope's film was reproduced by allowing the simulated intensity to saturate above a certain threshold value. Although not physical, a linear response of the film was assumed for simplicity. The simulated pattern accounts for radial broadening due to coherence length. It does not account for angular broadening due to the curvature of the lattice axis, perceived broadening due to halation, or slight variations in  $C_{60}$ - $C_{60}$  separations that would tend to annihilate high- $Q$  reflections.

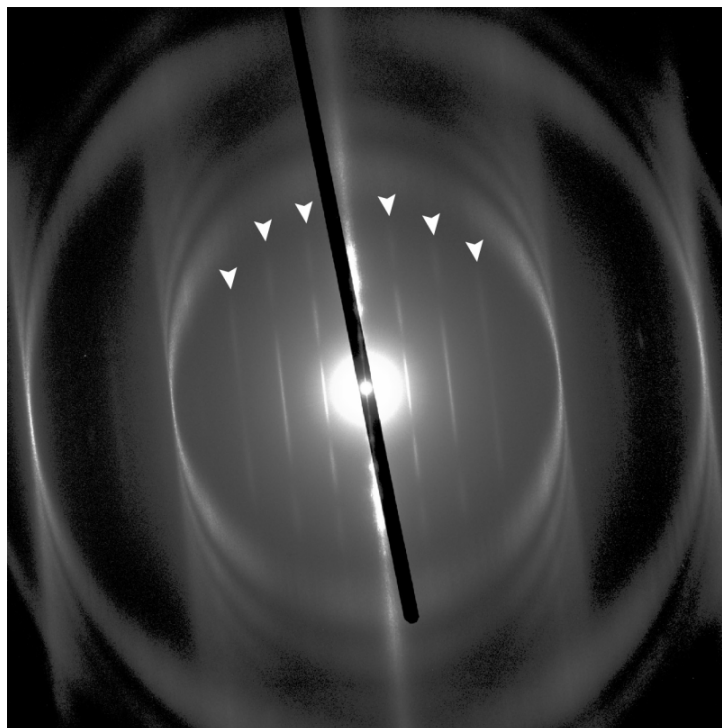


**Figure 1.** SAD pattern of an isolated SWNT rope, where the tubes are filled with  $C_{60}$ . The meridian is oriented approximately horizontally. The meridional reflections (arrows) are spaced by  $0.63 \text{ \AA}^{-1}$ , corresponding to a lattice periodicity of 1.00 nm.

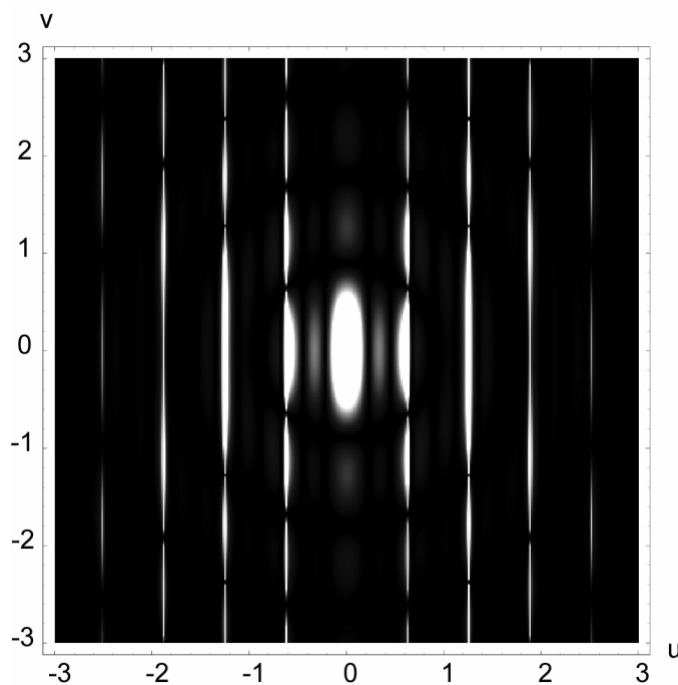


**Figure 2.** Simulated SAD pattern of a simple lattice of  $C_{60}$ . Empirical patterns show the same streaks with nodes and subsidiary maxima.

The simulation predicts the existence of streaks perpendicular to the meridian, spaced by  $0.63 \text{ \AA}^{-1}$ , and having nodes corresponding to the minima of  $j_0$ . All of these predictions are in excellent agreement with the experimental patterns, which show streaks with subsidiary maxima in the correct positions. Intensity decays at high-Q due to the decay of both the atomic form factor  $f(Q)$  and the molecular form factor  $\phi(Q)$ . The consistency of the empirical SAD intensity with a that of a purely one-dimensional lattice indicates that there is no three-dimensional inter-tube ordering of the encapsulated  $C_{60}$ . Also of interest is the fact that fcc  $C_{60}$  has an orientational ordering transition that occurs at 260 K. It is possible that  $C_{60}$ @SWNT has an analogous transition. However, the agreement of experimental and simulated patterns (the former of which was recorded at 94 K, and the latter of which assumes a homogenous spherical shell) indicates that if rotational freezing has occurred, it has occurred in such a way that superlattice reflections do not exist or are not detected.

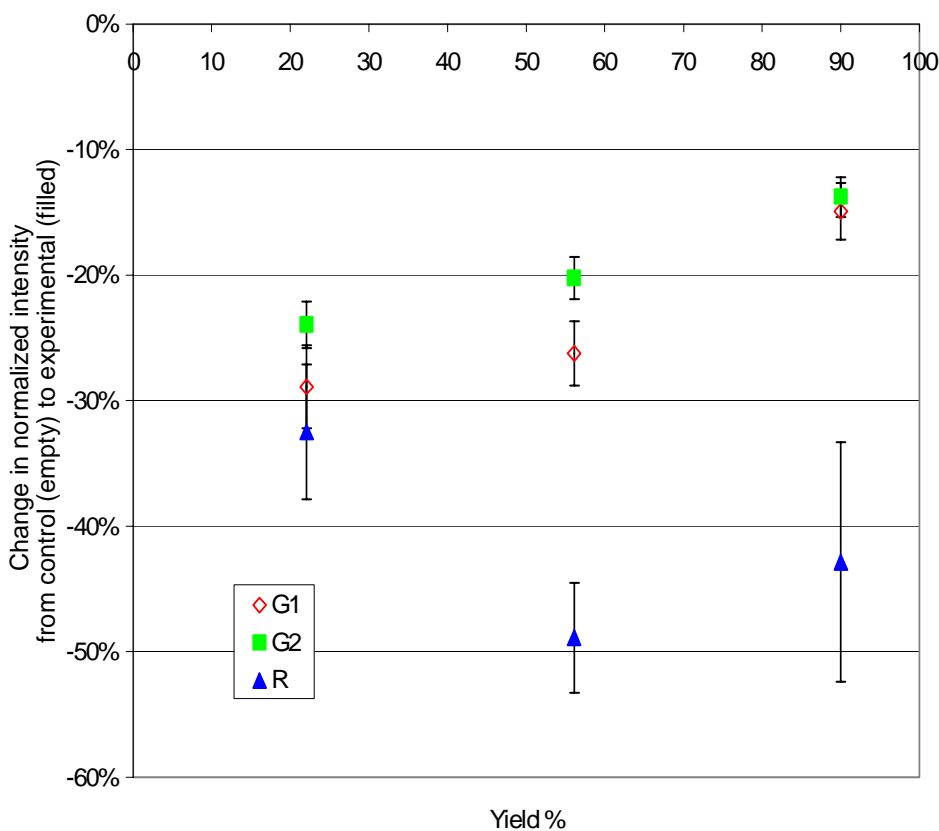


**Figure 3.** Change in average normalized Raman intensity as a function of  $C_{60}$ @SWNT yield. In general, material with filled SWNTs exhibited lower normalized intensities than material with empty SWNTs.

As described previously, Raman spectra were analyzed by comparing the average normalized intensities of the control and experimental samples from each processing condition. For all the tested conditions,  $G_1/D$ ,  $G_2/D$ , and  $R/D$  are greater for the control sample than for the experimental sample. The percent change in each ratio upon filling is plotted as a function of yield in Figure 3, with the error derived from one standard deviation of both control and experimental ratios. More data are required to draw any valid conclusions about the sensitivity of the various ratios to yield.

The differences between the control and experimental Raman spectra can be explained if the experimental samples experience either a relative increase in D or a relative decrease in  $G_1$ ,  $G_2$ , and R. If the D-band is affected, then the experimental sample should have a greater fraction of disordered carbon than the control, possibly due to disruption of the nanotubes' walls or decomposition and/or intercalation of  $C_{60}$  during the synthesis process. However, no evidence of this was detected by TEM. In fact, neglecting the presence of  $C_{60}@SWNT$ , the gross microstructures of the two samples in each control-experimental pair appeared nearly identical.

Alternatively, the normalized intensities may change due to a decrease in  $G_1$ ,  $G_2$ , and R. These peaks are associated with the SWNTs and are resonance-enhanced, so the decrease in intensity can be due to a change in the vibrational frequencies of the SWNTs and/or to a change in their corresponding electronic structure (Fermi level or density-of-states). Since the polyaromatic shells in the material also contribute to  $G_1$  and  $G_2$ , these two peaks should be less sensitive to changes in the SWNTs. This is consistent with the observed trend. Note the perturbation of the electronic structure of a SWNT by interior  $C_{60}$  has been directly detected [4], although we do not try to quantitatively reconcile our Raman data at present.

Curiously, despite the presence of large quantities of  $C_{60}$  in the experimental samples, the well defined Raman signature of  $C_{60}$  was never detected. It is possible that this is because the SWNTs shield interior  $C_{60}$  from incident radiation, thereby annihilating the fullerene's Raman cross-section. This problem is made more complicated by the fact that the resonance condition of each filled SWNT is potentially changed due to intermolecular hybridization, as has been shown by STM and STS [4]. Clearly, it is not necessarily the case that high yields of  $C_{60}@SWNT$  should give the Raman shifts expected from an isolated  $C_{60}$  molecule.

## CONCLUSION

Using empirical and simulated electron diffraction, the structure of  $C_{60}@SWNT$  was shown to be crystalline with a simple Bravais lattice. The endohedral  $C_{60}$  lattice is simple, with each  $C_{60}$  separated from its neighbors by the lattice parameter, 1.00 nm. The radial width of the Bragg reflections further evidences the extent of filling. Characterization by Raman spectroscopy suggests that the vibronic states of  $C_{60}@SWNT$  might be different than those of an empty SWNT.

## REFERENCES

1. B.W. Smith, M. Monthieux D.E. Luzzi, *Nature*, **396**, 323 (1998).
2. B.W. Smith D.E. Luzzi, *Chem. Phys. Lett.*, **321**, 169 (2000).
3. A.M. Rao et al., *Science*, **275**, 187 (1997).
4. D.J. Hornbaker et al., *Science* **295**, 828 (2002).